MOLECULAR DETERMINANTS OF GINKGOLIDE BINDING IN THE GLYCINE RECEPTOR PORE

Rebecca Hawthorne[1] Brett A. Cromer[2], Hooi-Ling Ng[2], Michael W. Parker[2] and Joseph W. Lynch[1]

[1] School of Biomedical Sciences, University of Queensland, Brisbane, QLD 4072, Australia

[2] St. Vincent's Institute of Medical Research, 9 Princes St. Fitzroy, Victoria, 3065, Australia

Address correspondence to: Dr. Joseph Lynch, School of Biomedical Sciences, University of Queensland, Brisbane, QLD 4072, Australia. Tel. +617 3365 3157; Fax. +617 3365 1766; Email: j.lynch@uq.edu.au

Abbreviations: BB, bilobalide; EC_{50}, half-maximal concentration for activation; LGIC, ligand-gated ion channel; GA, ginkgolide A; $GABA_AR$, γ-aminobutyric acid type-A receptor chloride channel; GB, ginkgolide B; GC, ginkgolide C; GlyR, glycine receptor chloride channel; IC_{50}, half maximal concentration for inhibition; I_{max}, saturating current magnitude; M1, first transmembrane domain; M2, second transmembrane domain; nAChR, nicotinic acetylcholine receptor cation channel; n_H, Hill coefficient; PTX, picrotoxin; WT, wild type.

Abstract: Ginkgolides are potent blockers of the glycine receptor Cl^- channel (GlyR) pore. We sought to identify their binding sites by comparing the effects of ginkgolides A, B and C and bilobalide on α1, α2, α1β and α2β GlyRs. Bilobalide sensitivity was drastically reduced by incorporation of the β subunit. In contrast, the sensitivities to ginkgolides B and C were enhanced by β subunit expression. However, ginkgolide A sensitivity was increased in the α2β GlyR relative to the α2 GlyR but not in the α1β GlyR relative to the α1 GlyR. We hypothesised that the subunit-specific differences were mediated by residue differences at the second transmembrane domain 2' and 6' pore-lining positions. The increased ginkgolide A sensitivity of the α2β GlyR was transferred to the α1β GlyR by the G2'A (α1 to α2 subunit) substitution. In addition, the α1 subunit T6'F mutation abolished inhibition by all ginkgolides. As the ginkgolides share closely-related structures, their molecular interactions with pore-lining residues were amenable to mutant cycle analysis. This identified an interaction between the variable R2 position of the ginkgolides and the 2' residues of both α1 and β subunits. These findings provide strong evidence for ginkgolides binding at the 2' pore-lining position.

Running title: Glycine receptor ginkgolide binding

Keywords: mutant cycle analysis, channel block, ligand-gated ion channel, *Ginkgo biloba*, patch clamp electrophysiology.

Extracts prepared from the leaves, roots and bark of the *Ginkgo biloba* tree are among the most widely used herbal medicines worldwide. They have been used to treat a number of conditions including cerebrovascular and neurodegenerative disorders (Le Bars *et al.* 1997; Maclennan *et al.* 2002; Ahlemeyer and Krieglstein 2003). *G. biloba* extracts contain several terpene trilactone compounds that are believed to be the major active constituents. The most abundant of these are ginkgolides A, B and C (GA, GB and GC) and bilobalide (BB) (van Beek 2005). GB has long been known as a platelet activating factor antagonist (Sanchez-Crespo *et al.* 1985). However, until recently there have been few insights into the molecular basis of the central nervous system effects of these compounds.

GB was recently discovered to be a specific and potent pore blocker of the glycine receptor chloride channel (GlyR) with an IC_{50} of 0.27 μM (Kondratskaya *et al.* 2002). Subsequent studies investigated the rank order of potency of ginkgolides and BB at the GlyR (Chatterjee *et al.* 2003; Ivic *et al.* 2003) and the GlyR subunit-dependence of GB inhibition (Kondratskaya *et al.* 2004). A limitation of each of these studies is that they were performed on cultured hippocampal or cortical neurons where the GlyR subunit composition was unknown. Nevertheless, these studies implicated GB as a subunit-specific blocker of the GlyR, with a preference for β subunit-containing receptors. This conclusion has recently been confirmed on homomeric α and heteromeric αβ GlyRs recombinantly expressed in *Xenopus* oocytes (Kondratskaya *et al.* 2005). Interestingly, the earlier studies showed that GA was significantly less potent than GB or GC (Chatterjee *et al.* 2003; Ivic *et al.* 2003), despite the 3 compounds sharing a highly conserved molecular structure (Fig. 1).

GlyRs mediate inhibitory neurotransmission in the adult rat spinal cord and brainstem (Lynch 2004). They are anion-selective channels that belong to the pentameric cysteine-loop family of ligand-gated ion channels (LGICs), of which the nicotinic acetylcholine receptor cation channel (nAChR) is the prototypical member. To date, 5 GlyR subunits have been identified (α1-α4, β). Embryonic receptors generally comprise α2 homomers or α2β heteromers, whereas the dominant adult subtype is the α1β heteromer (Lynch 2004). Heteromeric GlyRs are believed to exist in a 2α:3β stoichiometry (Grudzinska *et al.* 2005), with the β subunit responsible for anchoring GlyRs to postsynaptic densities via the cytoplasmic protein, gephyrin (Kneussel and Betz 2000). The α1, α2 and α3 subunits exhibit

differential synaptic distribution patterns that are particularly evident in the superficial dorsal horn of the spinal cord (Harvey *et al.* 2004) and in the retina (Haverkamp *et al.* 2003; Haverkamp *et al.* 2004). The physiological consequences of the differential distribution patterns are difficult to establish as there are currently few pharmacological probes that can effectively discriminate among β subunit-containing GlyR isoforms (Lynch 2004).

In an attempt to redress this situation and to understand the molecular basis of ginkgolide inhibition, the present study systematically investigated the specificity of GA, GB, GC and BB for recombinantly expressed α1, α2, α1β and α2β GlyRs. Furthermore, because GA and GB exhibit significant differences in GlyR sensitivity despite differing in structure by only a single atom (Fig. 1), we reasoned that it might be possible to establish the molecular basis of the subunit specificity of these compounds. Accordingly, the second aim of this study was to employ mutant cycle analysis to identify specific interactions between non-conserved GlyR pore-lining residues and structurally-divergent molecular groups of the ginkgolides.

Materials and Methods

Mutagenesis and expression of GlyR cDNAs

The human GlyR α1 subunit cDNA was subcloned into the pCIS2 plasmid vector. The human α2 subunit, which was kindly provided by Dr Paul Groot-Kormelink (University College, London), was subcloned into the pcDNA3.1 plasmid vector. The human β subunit was subcloned into the pIRES2-EGFP plasmid vector (Clontech, Palo Alto, CA, USA). Site-directed mutagenesis was performed using the QuickChange mutagenesis kit (Stratagene, La Jolla, CA, USA) and the successful incorporation of mutations was confirmed by sequencing the clones. HEK293 cells were transfected using a calcium phosphate precipitation protocol. When co-transfecting the GlyR α and β subunits, their respective cDNAs were combined in a ratio of 1:20. After exposure to transfection solution for 24 hrs, cells were washed twice using the culture medium and used for recording over the following 24 - 72 hrs.

Electrophysiology

The cells were observed using a fluorescent microscope and currents were measured using the whole cell patch-clamp configuration. Cells were perfused by a control solution that contained (in mM): 140 NaCl, 5 KCl, 2 $CaCl_2$, 1 $MgCl_2$, 10 HEPES, 10 glucose, with the pH adjusted to 7.4 with NaOH. Patch pipettes were fabricated from borosilicate hematocrit tubing (Vitrex, Modulohm, Denmark) and heat polished. Pipettes had a tip resistance of ~ 1.5 MΩ when filled with the standard pipette solution which contained (in mM): 145 CsCl, 2 $CaCl_2$, 2 $MgCl_2$, 10 HEPES, 10 EGTA, with the pH adjusted to 7.4 with NaOH. After establishment of the whole cell configuration, cells were voltage-clamped at –40 mV (unless otherwise indicated) and membrane currents were recorded using an Axopatch 1D amplifier and pCLAMP9 software (Axon Instruments, Union City, CA, USA). The cells were perfused by a parallel array of microtubular barrels through which solutions were gravity-induced. All experiments were conducted at room temperature (19 – 22 ^{o}C).

GFP fluorescence was used to identify cells expressing the GlyR β subunit. The successful incorporation of β subunits into functional receptors was inferred by their characteristic reduction in picrotoxin sensitivity (Pribilla *et al.* 1992; Handford *et al.* 1996) as demonstrated in Table 2.

GA, BB and picrotoxin (PTX) were obtained from Sigma (St Louis, MO, USA). GB and GC were obtained from Biomol (Plymouth Meeting, PA, USA) and MP Biomedicals (Eschwege, Germany), respectively. PTX was stored frozen as a 100 mM stock in dimethylsulfoxide. Ginkgolides and BB were stored frozen as 10 mM stocks in dimethyl-sulfoxide.

Data Analysis

Results are expressed as mean ± standard error of the mean of 3 or more independent experiments. The Hill equation was used to calculate the saturating current magnitude (I_{max}), half-maximal concentration (EC_{50}) and Hill coefficient (n_H) values for glycine activation. A similar equation was also used to calculate the half maximal concentrations for inhibition (IC_{50}) and n_H values of the antagonists tested in this study. All curves were fitted using a non-linear least squares algorithm (Sigmaplot 9.0, Jandel Scientific, San Rafael, CA, USA). Statistical significance was determined by paired or unpaired Student's t-test, as appropriate, with $P < 0.05$ representing significance.

Homology modelling and compound docking

LGIC subunits comprise a large extracellular N terminal domain followed and a cluster of 4 α-helical transmembrane domains (M1-M4). The residue at the putative intracellular boundary of the pore-lining M2 domain is assigned position 1', and the outermost residue of this domain is assigned 19'. SwissPDB viewer (Guex and Peitsch 1997) was used to build a model of the GlyR α1 subunit M1 and M2 domains by homology with the equivalent region of the nAChR α subunit in the electron microscopy-derived closed-channel structure (pdb code 1OED) (Miyazawa *et al.* 2003). The M1-M2 loop was constructed from a loop database due to the presence of an extra residue relative to the 1OED template. M1 was included in the model to constrain the M1-M2 loop. As M1 does not directly line the pore, however, only the region from -2' to 19' of M2, including part of the M1-M2 loop, was assembled into a homopentameric model on the scaffold of the five M2 regions in 1OED. Side-chain clashes were removed by energy minimisation. AutoDock 3.0 (Morris and Olsen 1998) was used to explore the possible interactions of ginkgolides with the central pore region of the model. The Lamarckian genetic algorithm was used to produce 100 conformations of each ligand, which were clustered within a root-mean-squared deviation of 1.8 Å. Docked conformations of the ligands were inspected using VMD version 1.8 (Humphrey *et al.* 1996).

Results

Subunit-sensitivity of recombinant GlyRs to ginkgolides and BB

This study compared the effects of extracellularly-applied GA, GB, GC, BB and PTX on recombinantly expressed α1, α2, α1β and α2β GlyRs. The mean glycine I_{max}, EC_{50} and n_H values for each of the 4 receptor subtypes are summarised in Table 1. All values are within the range as measured previously for these receptors (Shan *et al.* 2001; Miller *et al.* 2004). We then measured the steady-state inhibitory dose-response of each test compound at each receptor. Compounds were applied at an EC_{50} glycine concentration as determined empirically for each receptor subunit composition. Examples of the inhibitory responses induced by 10 μM of each compound at each of the 4 receptor subtypes are shown

in Fig. 2A. The averaged dose-responses for GA, GB, GC and BB are displayed in Fig 2B. The averaged IC_{50} and n_H values of best fit for these compounds and PTX are displayed in Table 1.

The IC_{50} values for GA did not differ significantly among the α1, α2 and α1β GlyRs. However, the GA sensitivity of the heteromeric α2β GlyR was significantly increased relative to the homomeric α1 and α2 GlyRs (Table 2).

The averaged dose-responses for GB and GC revealed a different pattern of subunit-dependence (Fig. 2B, Table 2). The sensitivity of both compounds was significantly increased in the α1β heteromer relative to the α1 homomer and in the α2β heteromer relative to the α2 homomer (Table 2). The homomeric α1 and α2 GlyRs were equally GC. However, the α1 GlyR was slightly more sensitive than the α2 GlyR to GB, but this was not statistically significant. Although Kondratskaya *et. al.* (2005) also found that β subunit incorporation increased GB potency, they found the α1 homomer to be significantly more sensitive than the α2 homomer to GB inhibition. This difference may relate to the expression system: they used *Xenopus* oocytes whereas the present study was performed on HEK293 cells.

The subunit-sensitivity of BB showed a dramatically different profile. BB discriminated relatively weakly between the α1 and α2 homomeric GlyRs, although the α2 was significantly more sensitive to BB inhibition (Fig. 2B, Table 2). Incorporation of the β subunit caused a drastic reduction in the BB sensitivities of both α1β and α2β GlyRs (Table 2). The effects of PTX, which have already been characterised at these receptors (Pribilla *et al.* 1992; Lynch *et al.* 1995; Handford *et al.* 1996), are included as a control (Table 2). We found the α2 homomer to be significantly more sensitive than the α1 homomer to PTX inhibition. However, as with BB, incorporation of the β subunit dramatically reduced the PTX sensitivity of both α1β and α2β GlyRs. Thus, BB and PTX exhibit qualitatively similar patterns of subunit-dependence.

The above experiments quantitated the effects of extracellularly-applied ginkgolides. We also sought to determine whether these compounds were active from the internal membrane surface. With 30 μM GA in the patch pipette, we found that the magnitude of whole-cell glycine-gated currents did not change significantly during the first 10 min of whole-cell recording (n = 3 cells, data not shown). We therefore conclude that ginkgolides access their site from the extracellular surface only.

Functional properties of inhibition by ginkgolides and BB

GB has previously been proposed as a pore-blocker of a native hippocampal neuron GlyR based on its glycine-independent, voltage-dependent and use-dependent properties (Kondratskaya *et al.* 2002). GC has also been shown to inhibit a native cortical neuronal GlyR in a use-dependent manner (Ivic *et al.* 2003). In the present study, we systematically investigated the voltage-dependence, glycine concentration-dependence and use-dependence of GA, GB, GC, BB and PTX at the α2 homomeric GlyR. The α2 GlyR was chosen for analysis as the four *G. biloba* derivates showed approximately equal efficacy at this receptor (Table 2). As a final test, we determined whether GA could be 'trapped' in the pore of the R271C GlyR in the closed state (Hawthorne and Lynch 2005).

To investigate voltage dependence, we activated the GlyRs with an EC_{50} glycine concentration and compared the percentage inhibition induced by 10 μM of each compound at -40 and +40 mV. Sample recordings (Fig. 3A) suggest that GA inhibition is voltage-dependent whereas BB inhibition is not. The pooled results, summarised in Fig. 3B, reveal that inhibition by GA, GB and GC is significantly increased at depolarised potentials, whereas BB and PTX displayed no voltage-dependence. We were unable to establish from the literature which of the *G. biloba* compounds are charged in a physiological saline at pH 7.4. Assuming these compounds bind in the pore (see below), the voltage dependence of their inhibition implies that GA, GB and GC possess a net negative charge whereas picrotoxin and BB are uncharged.

We then investigated the glycine concentration dependence of inhibition. In this experiment, the inhibition induced by 10 μM of each compound was compared at an EC_{50} (50 μM) glycine concentration and a near-saturating (200 μM) glycine concentration. Sample traces for GB and BB (Fig. 4A) suggest that GB inhibition is insensitive to glycine concentration, whereas BB inhibition decreases as glycine concentration is increased. The pooled results, summarised in Fig. 4B, reveal that inhibition by GA, GB and GC is glycine-independent, whereas inhibition by BB and PTX is reduced as glycine concentration is increased.

The use-dependence of the compounds was investigated as shown in Fig. 5A. The left and right panels show the effects of 10 μM GA applied in the open and closed states, respectively. As seen in the left panel, the rate of current recovery following GA removal is slower than the control rate of glycine-

induced activation, due to the slow dissociation of GA. If GA can access its site equally well in the open and closed states, the rate at which glycine activates the channels immediately after a closed state GA application should be slowed to a similar extent. To facilitate comparison of glycine activation rates, single exponentials were fitted to the curves indicated by numbers 1, 2 and 3 with averaged time constants for GA, GB, GC and BB presented in Fig. 5B. For all compounds tested, unbinding of the compound slowed glycine activation rate when applied in the open state but not when applied in the closed state. These data demonstrate that when applied in the closed state, the compounds either do not reach the inhibitory site or bind with relatively low affinity. Thus, all four compounds are use-dependent inhibitors of the α2 GlyR. A similar analysis previously showed that PTX inhibition was not use-dependent (Lynch *et al.* 1995).

We recently showed that PTX and BB are 'trapped' in the pore of the $\alpha1^{R271C}$ GlyR in the closed state (Hawthorne and Lynch 2005). The $\alpha1^{R271C}$ GlyR was employed as the effect is not apparent in the unmutated GlyR. We reasoned that if GA is a pore blocker then it should exhibit similar trap behaviour. To investigate this, we activated the $\alpha1^{R271C}$ GlyR with a 20 mM (saturating) concentration of glycine, then applied 10 mM GA in the open state, and determined its rate of unblock in the closed and open states. Fig. 6A shows an example of the effect of applying GA in the continuous presence of glycine. If glycine and GA are simultaneously removed once GA block has reached steady state, it is apparent that recovery from GA inhibition does not commence until glycine is re-applied 60 s later (Fig. 6B). This indicates that GA is 'trapped' in the closed state. When GA is applied in the closed state, a subsequent glycine application reveals that it does not reach its inhibitory site (Fig. 6C). Similar results were recorded in each of 4 cells. To quantitate these data, Fig. 6D shows the average percentage of original glycine current that was observed 65 s after the termination of the original glycine application under each of the experimental conditions depicted in Fig. 6A-C. The 0 and 65 s time points are indicated in Fig. 6A-C by the vertical dashed lines. Fig. 6D shows that the only condition that results in significant block at the 65 s time point is when GA is trapped in the closed state for 60 s.

In agreement with previous reports (Kondratskaya *et al.* 2002; Ivic *et al.* 2003), the results of these functional assays provide a strong case for ginkgolides binding in the pore. Because BB inhibition decreases as glycine concentration increases, it cannot be regarded as a classical pore blocker.

Molecular determinants of ginkgolide inhibition

Several studies have shown that the PTX sensitivity of anionic LGICs is sensitive to mutations at the 2' and 6' pore-lining positions (Ffrench-Constant *et al.* 1993; Gurley *et al.* 1995; Wang *et al.* 1995; Xu *et al.* 1995; Zhang *et al.* 1995; Etter *et al.* 1999; Shan *et al.* 2001). We previously demonstrated that the GlyR $\alpha1 \rightarrow \beta$ subunit mutation, G2'P, significantly increased the PTX sensitivity of homomeric $\alpha1$ GlyRs (Shan *et al.* 2001). We have also shown that the $\alpha1 \rightarrow \beta$ subunit substitution, T6'F, drastically reduced the sensitivity of homomeric $\alpha1$ GlyRs to both PTX and BB (Shan *et al.* 2001; Hawthorne and Lynch 2005). Given these findings, we hypothesized that ginkgolides inhibit GlyRs by blocking the channel in the 2' - 6' region and that subunit-specific differences in sensitivity are most likely due to residue differences at these positions.

A sequence alignment of the $\alpha1$, $\alpha2$ and β subunit M2 domains is shown in Fig. 7A, highlighting the differences at the 2' and 6' positions. As the minimum diameter of a GlyR open channel is about 6 Å (Fatima-Shad and Barry 1993; O'Mara *et al.* 2005) and structural data for the nAChR channel suggest a similar diameter at the 2' position (Miyazawa *et al.* 2003), it is not clear whether it is feasible for ginkgolides, with a minimum diameter of 8.9 Å (Zhao *et al.* 2002), to access this position in the channel pore. To examine the feasibility of this blocking site, we built a model of the pentameric $\alpha1$ GlyR M2 region and part of the M1-M2 loop by homology with the nAChR channel structure (Miyazawa *et al.* 2003). We then used in-silico docking to investigate the possibility of ginkgolides binding within the pore.

The docking results indicated that ginkgolide binding was possible at a number of sites in the pore but, based on lowest estimated energy and greatest clustering of docks, by far the best site was adjacent to the 2' and 6' positions, as shown for GA in Fig. 7B. Other possible sites indicated by docking were mostly near the extracellular mouth of the channel. Interestingly, no docking sites were found near the conserved L9' residue at the pore midpoint. This is consistent with a narrow constriction at the 9' position that is too narrow to accommodate a ginkgolide. This constriction presumably restricts access to and from the 2'-6' positions in the closed state. Although our model is based on a closed state conformation, the conformational changes associated with channel opening in the nAChR appear relatively subtle in this region (Unwin 1995). Consequently, our data support the feasibility of

ginkgolides blocking the open GlyR pore at the 2'- 6' region. Given the uncertainties of our GlyR model, especially in our use of a loop database to model the M1-M2 loop, we have not attempted to use docking to predict specific interactions between ginkgolides and the channel-lining groups. Rather we have used site-directed mutagenesis of the 2' and 6' residues to further investigate such potential interactions.

As the α1 subunit T6'F mutation drastically reduced the potency of both PTX and BB (Hawthorne and Lynch 2005), we hypothesised it should have a similar effect on the sensitivity to GA, GB and GC. Indeed, as shown in Fig. 7C, the sensitivity to all 3 ginkgolides was abolished in the $\alpha1^{T6'F}$ GlyR. Thus, a ring of 5 phenylalanines at the 6' pore-lining position dramatically disrupts inhibition by ginkgolides, BB and PTX. However, as ginkgolide sensitivity is actually increased in the presence of the β subunit (Table 2), it appears that any negative effect of the 6' phenylalanines must be minor provided that they are restricted to the β subunit in αβ heteromers. Moreover, despite the α1β and α2β GlyRs having no variation in structure at the 6' position, the ginkgolides display significant differences in sensitivity between these receptors (Table 2). These observations suggest that ginkgolide specificity is dominated by other subunit-specific differences, with the 2' residues being obvious candidates. These experiments rule out the possibility that the β subunit F6' may be a binding site. However, it remains possible that the α subunit T6' residues could contribute to ginkgolide coordination.

Since the wild type (WT) homomeric α1 and α2 GlyRs exhibit similar sensitivities to all 3 ginkgolides (Table 2), it is unlikely that the G2'A (α1 → α2 subunit) substitution will significantly affect the ginkgolide sensitivity of homomeric α1 GlyRs. We have previously shown that this mutation has no effect on glycine sensitivity (Table 1). As anticipated, the homomeric α1, α2 and $\alpha1^{G2'A}$ GlyRs all exhibited similar GA sensitivities (Fig. 7D, left panel). The mean IC_{50} and n_H values for GA at the $\alpha1^{G2'A}$ GlyR were 3.0 ± 0.6 μM and -0.9 ± 0.1 (both n = 4), respectively. These values did not differ significantly from their respective values at the α1 GlyR. However, we demonstrated above that incorporation of the β subunit increased GA sensitivity in the α2β GlyR but not in the α1β GlyR (Table 2). This prompts the hypothesis that the G2'A substitution may increase GA sensitivity in $\alpha1^{G2'A}\beta$ heteromers relative to the α1β heteromers. Fig. 7D (right panel) shows the averaged dose-response for GA at the heteromeric $\alpha1^{G2'A}\beta$ GlyR. The mean IC_{50} and n_H values were 1.4 ± 0.3 μM and -1.0 ± 0.1 (both n = 4), respectively. The mean IC_{50} was significantly lower than the mean α1β GlyR value (P <

0.01) but not significantly different to the mean α2β GlyR value. Thus, the increased GA sensitivity of the α2β GlyR over the α1β GlyR is mediated by the G2'A (α1 → α2 subunit) substitution. A recent study showed that the α1 subunit G2'A mutation reduced GB sensitivity to the level seen in the α2 GlyR (Kondratskaya *et al.*, 2005).

As noted above, introduction of the β subunit increases the potency of GB and GC (Table 2). As this effect is independent of which α subunit is present, we hypothesised it was due to the introduction of the β subunit prolines at the 2' position. If so, the effect might be mimicked by introducing the G2'P (α1 → β) mutation into the homomeric α1 GlyR. We have previously shown that this mutation increases the glycine EC_{50} value to around 150 μM (Table 1). Averaged dose-responses for GA, GB, GC and BB at the $\alpha1^{G2'P}$ GlyR, measured in the presence of an EC_{50} glycine concentration, are displayed in Fig. 8 and the averaged parameters of best fit are presented in Table 2. The corresponding dose-response curves at the WT α1 GlyR, reproduced from Fig. 2, are included in Fig. 8 as dashed lines. These results show that the G2'P mutation caused modest, but significant, increases in sensitivity to BB and GC, but dramatic decreases in sensitivity to GA and GB.

Clearly, the G2'P mutation in the α1 homomer does not replicate the effect on ginkgolide sensitivity of adding the β subunit. There does, however, appear to be a trend whereby the presence of prolines at the 2' position improves the relative affinity for GC over GB and for GB over GA. To investigate further the role of the 2' residues in determining ginkgolide sensitivity, we compared the potencies of GA, GB and GC on WT α1β GlyRs with their effects on the $\alpha1\beta^{P2'G}$, $\alpha1^{G2'P}\beta$, and $\alpha1^{G2'P}\beta^{P2'G}$ mutant GlyRs. The results of these experiments are summarised in Table 3. Note that in some cases, receptor sensitivity to ginkgolides was so low that IC_{50} values could not be measured. These data indicate that the affinity for ginkgolides is not determined simply by the number of 2'P residues but the apparent trend of 2'P residues improving the relative affinity for GC over GB over GA does seem to be maintained. As GA, GB and GC are identical except for the presence, respectively, of 0, 1 or 2 hydroxyl groups at the R1 and R2 positions (Fig. 1), the effect of 2' mutations on relative ginkgolide affinity hints at a direct interaction with this residue. To further examine the evidence for such an interaction, we applied double-mutant cycle analysis to our data.

Mutant cycle analysis

Mutant cycle analysis has been widely used to investigate interactions between pairs of residues in proteins (Hidalgo and MacKinnon 1995; Schreiber and Fersht 1995; French and Dudley 1999) or between protein residues and molecular groups on non-peptide ligands (Penzotti *et al.* 2001; Yan and White 2005). In the latter case, the effect on ligand affinity of changing a ligand group or a protein residue, either individually or both together, is measured. If the individual effects are independent and additive, indicating no effective interaction between the two groups, then the coupling coefficient (Ω), defined in eq. 1 below, will be equal to one.

$$\Omega = \frac{(IC50_{WT,\,L1}).(IC50_{MUT,\,L2})}{(IC50_{WT,\,L2}).(IC50_{MUT,\,L1})} \qquad \text{(eq. 1)}$$

The subscripts WT and MUT represent the wild type and mutant receptor, respectively, and L1 and L2 denote the two ligands being compared. Note that ligand affinities rather than IC_{50}s are normally used in this equation. However, we assume that these two quantities are equivalent for non-competitive antagonists such as ginkgolides. Values of $\Omega > 2.5$ have been shown to identify direct interactions between molecular groups (Schreiber and Fersht 1995). The interaction energy, $\Delta\Delta G_{int}$, between the two substituted groups is given by $RT\ln\Omega$, where R is the gas constant and T is temperature.

GA and GB differ in structure by a single group at position R1, with a hydrogen in GA replaced by a hydroxyl in GB (Fig. 1). Similarly, GC differs from GB by substitution of a hydrogen with a hydroxyl at position R2 (Fig. 1). Consequently, double-mutant cycle analysis of the IC_{50}s for GB versus GA or GC versus GB at WT versus 2' mutant GlyRs reports on possible interactions between the 2' residue and the R1 or R2 positions, respectively. Fig. 9 shows the mutant cycles that we analysed, with Ω values and interaction energies in the centre of each cycle. The arrows indicate the starting and finishing point for each cycle. For ease of comparison, we have defined receptors with all glycines at 2' as the starting point for each cycle so effectively a G → P substitution is always considered. Likewise, GC is used as L1 (starting point) relative to GB as L2 and GB as L1 relative to GA as L2. Thus removal of a

hydroxyl is always tested. Note that not all of the IC_{50} data could be included in mutant cycle analysis as some cycles could not be completed due to an incomplete data set.

As shown in Fig. 9, mutant cycle analysis provides evidence for an interaction between the ginkgolide R1 position and the 2' position in α1 homomers (Fig. 9A, cycle 2) but the interaction energy is relatively weak and there is no evidence for such an interaction in α1β heteromers. Much more convincing is the consistent evidence for a stronger interaction between the ginkgolide R2 position and the GlyR 2' position in both α1 homomers (Fig. 9A, cycle 1) and α1β heteromers (Fig. 9B). This occurs regardless of whether the 2' substitution is in the α1 subunit (cycle 5) or β subunit (cycle 3). In all cases, a G2'P substitution improves the relative affinity for GC over GB, indicating a positive interaction between the R2 hydroxyl in GC and a 2'P that is not present with a 2'G. This provides strong supporting evidence that the ginkgolide-binding site is adjacent to the 2' position in the GlyR open pore.

Discussion

Subunit-sensitivity of inhibition by ginkgolides and BB

This study has demonstrated that GA, GB and GC are subunit-selective inhibitors of recombinant GlyRs. There was no significant difference in sensitivity between α1 and α2 homomeric GlyRs to any of the three compounds. However, both the α1β and α2β GlyRs show a significantly increased sensitivity to GB and GC, relative to their respective homomers. On the other hand, GA sensitivity is increased in the α2β GlyR relative to the α2 GlyR but not in the α1β GlyR relative to the α1 GlyR. Thus, together these compounds are able to distinguish α1 from α2 subunit-containing αβ GlyRs and can discern the presence of the β subunit. Ginkgolides may therefore be useful as pharmacological probes for identifying the subunit composition of synaptic GlyRs.

These results are largely consistent with previous results from native GlyRs expressed in cultured hippocampal neurons. Hippocampal GlyRs showed an age-dependent increase in GB sensitivity that coincided with a decreased PTX sensitivity (Kondratskaya *et al.* 2004). This strongly suggests that the increased GB sensitivity was mediated by a switch in GlyR stoichiometry from α homomeric to αβ heteromeric. Adult hippocampal neuronal GlyRs, which are most likely α1β heteromers (Lynch 2004),

showed a relatively high sensitivity to GB and GC but a lower sensitivity to GA (Chatterjee *et al.* 2003). However, a significant point of difference is that the adult hippocampal GlyRs were 5 – 10 times more ginkgolide-sensitive (Kondratskaya *et al.* 2002; Chatterjee *et al.* 2003; Kondratskaya *et al.* 2004) than the recombinant α1β GlyRs examined here. The basis for this difference is not yet known. A report published after completion of this study found that the GB sensitivity of GlyRs recombinantly expressed in *Xenopus* oocytes is also increased in the presence of the β subunit (Kondratskaya *et al.* 2005).

The subunit-selectivity of BB inhibition of the GlyR has not previously been investigated. This study reveals BB to be modestly selective for homomeric α2 GlyRs over α1 GlyRs, but highly selective for α homomers over αβ heteromers. The inhibitory properties of GA, GB, GC and BB have recently been investigated at recombinantly-expressed α1β2γ2L $GABA_A$Rs (Huang *et al.* 2003; Huang *et al.* 2004). BB was the most potent of these compounds with an IC_{50} value near 5 μM. similar to the GlyR, ginkgolides inhibited the α1β2γ2L $GABA_A$R in a manner that was non-competitive with agonist. On the other hand, BB inhibition displayed elements of both competitive and non-competitive antagonism (Huang *et al.* 2003).

Molecular determinants of ginkgolide inhibition

The functional properties of ginkgolide inhibition, summarised in Figs. 3-6, suggest a binding site deep within the open channel pore. Our modelling and docking results support the feasibility of a binding site in the pore adjacent to the 2' and 6' positions, a location that is strongly supported by our site-directed mutagenesis data. We show that the $\alpha1^{T6'F}$ mutation abolishes ginkgolide sensitivity and that a Gly for Ala substitution at the 2' position is responsible for the differential GA sensitivity of α1β and α2β GlyRs. Further strong support for a binding site adjacent to the 2' position comes from mutant cycle analysis of the relative sensitivity to GA, GB and GC of α1 and α1β GlyRs. This analysis revealed a significant interaction between the ginkgolide R2 position and the 2' residues in α1 homomers and in both α1 and β subunits of α1β heteromers (Fig. 9). In all cases this interaction was positive with a hydroxyl at the R2 position and proline at the 2' position.

Substitution of proline by glycine is non-conservative. Nevertheless, we rule out the idea that proline causes a non-specific structural change in the pore as this would not be expected to discriminate

between large molecules that differ in structure by a single atom. Apart from removing a bulky side-chain, the P2'G substitution may affect backbone conformation. Consequently, it is difficult to predict the nature of interactions disrupted by such substitutions. Nevertheless, several considerations are worthy of discussion. The magnitudes of the calculated interaction energies (Fig. 9) suggest the existence of van der Waals interactions between the R2 hydroxyl and the 2'P side-chain. Alternatively, the R2 hydroxyl could contribute to a hydrogen bond but no hydrogen bonds are available directly with a proline side-chain. Hydrogen bonds with the channel near the 2' position may, however, be indirectly disrupted by a P2'G substitution. Firstly, the 2' backbone nitrogen would become available as a hydrogen bond donor, and this may interact with a hydrogen bond acceptor on a side-chain located more cytoplasmic than the 2' position. Thus, if this putative acceptor interacts with the backbone nitrogen of a 2'G, substitution with a 2'P may make the acceptor available to interact with the R2 hydroxyl of GC, potentially explaining the mutant cycle results. This putative interaction with R2 is highly speculative because our GlyR channel model becomes less reliable around the cytoplasmic end of the pore due to the presence of extra residues relative to the nAChR template. Thus, the identity of the putative hydrogen bond acceptor cannot be predicted with any certainty. A second possibility is that P2'G substitutions may induce local conformational changes that reduce the availability of other hydrogen bonding side-chains, such as T6' residues, consistent with our T6'F mutant results.

Our mutant cycle analysis provides strong evidence for ginkgolides binding at the 2' position of the GlyR channel but it is beyond the limits of our current data and the accuracy of our channel model to predict the precise positioning and orientation of the bound ginkgolides. In a recent study, systematic modification of the hydroxyl groups on GC showed that all four hydroxyl groups on this compound are important for its inhibition of GlyRs (Jaracz *et al.* 2004). This provides further support for the role of hydroxyl groups in GC binding, emphasizes a probable role for hydrogen bonds and offers further opportunities for defining the binding interactions by mutant cycle analysis.

Molecular mechanism of BB inhibition

On the basis of its use-dependence, closed state trap and sensitivity to the T6'F mutation, we previously inferred that BB binds in the α1 GlyR pore (Hawthorne and Lynch 2005). We show here that incorporation of the β subunit increased GlyR sensitivity to ginkgolides but decreased GlyR sensitivity to

BB, implying substantial differences in their respective binding mechanisms. The present study has also shown that BB inhibition is similar to ginkgolide inhibition in that it is use-dependent. However, unlike the ginkgolides, BB inhibition is voltage-independent and shows competition with glycine. It will be interesting to establish the structural basis of these differences. Elucidation of the molecular basis of BB inhibition may provide insights into the pore structural rearrangements that accompany GlyR activation.

Summary

We have identified GA, GB, GC and BB as subunit-selective inhibitors of the GlyR. Using mutant cycle analysis we have provided strong evidence that ginkgolides bind in the pore at the level of the 2' pore-lining residues. The subunit-selectivity of ginkgolides can be partially explained by subunit-specific differences in amino acids at the 2' pore-lining position. Future experiments aimed at more precisely delineating the binding sites of ginkgolides and BB may place constraints on the pore conformation and side-chain exposure in the closed and open states.

Acknowledgements

This research was supported a grant from the Australian Research Council to J.W.L. and a grant from the National Health and Medical Research Council of Australia (NHMRC) to M.W.P. and B.A.C. M.W.P. and J.W.L. are both supported by NHMRC Research Fellowships. We thank Dr Tim Webb and Dr Craig J. Morton for useful suggestions and comments on the manuscript.

References

Ahlemeyer B. and Krieglstein J. (2003) Neuroprotective effects of Ginkgo biloba extract. Cell Mol Life Sci 60, 1779-1792.

Chatterjee S. S., Kondratskaya E. L. and Krishtal O. A. (2003) Structure-activity studies with Ginkgo biloba extract constituents as receptor-gated chloride channel blockers and modulators. Pharmacopsychiatry 36 Suppl 1, S68-77.

Etter A., Cully D. F., Liu K. K., Reiss B., Vassilatis D. K., Schaeffer J. M. and Arena J. P. (1999) Picrotoxin blockade of invertebrate glutamate-gated chloride channels: subunit dependence and evidence for binding within the pore. J Neurochem 72, 318-326.

Fatima-Shad K. and Barry P. H. (1993) Anion permeation in GABA- and glycine-gated channels of mammalian cultured hippocampal neurons. Proc Roy Soc Biol Sci 253, 69-75.

Ffrench-Constant R. H., Rocheleau T. A., Steichen J. C. and Chalmers A. E. (1993) A point mutation in a Drosophila GABA receptor confers insecticide resistance. Nature 363, 449-451.

French R. J. and Dudley S. C., Jr. (1999) Pore-blocking toxins as probes of voltage-dependent channels. Methods Enzymol 294, 575-605.

Grudzinska J., Schemm R., Haeger S., Nicke A., Schmalzing G., Betz H. and Laube B. (2005) The beta subunit determines the ligand binding properties of synaptic glycine receptors. Neuron 45, 727-739.

Guex N. and Peitsch M. C. (1997) SWISS-MODEL and the Swiss-PdbViewer: an environment for comparative protein modeling. Electrophoresis 18, 2714-2723.

Gurley D., Amin J., Ross P. C., Weiss D. S. and White G. (1995) Point mutations in the M2 region of the alpha, beta, or gamma subunit of the GABAA channel that abolish block by picrotoxin. Receptors Channels 3, 13-20.

Handford C. A., Lynch J. W., Baker E., Webb G. C., Ford J. H., Sutherland G. R. and Schofield P. R. (1996) The human glycine receptor beta subunit: primary structure, functional characterisation and chromosomal localisation of the human and murine genes. Brain Res Mol Brain Res 35, 211-219.

Harvey R. J., Depner U. B., Wassle H. et al (2004) GlyR alpha3: an essential target for spinal PGE2-mediated inflammatory pain sensitization. Science 304, 884-887.

Haverkamp S., Muller U., Harvey K., Harvey R. J., Betz H. and Wassle H. (2003) Diversity of glycine receptors in the mouse retina: localization of the alpha3 subunit. J Comp Neurol 465, 524-539.

Haverkamp S., Muller U., Zeilhofer H. U., Harvey R. J. and Wassle H. (2004) Diversity of glycine receptors in the mouse retina: localization of the alpha2 subunit. J Comp Neurol 477, 399-411.

Hawthorne R. and Lynch J. W. (2005) A picrotoxin-specific conformational change in the glycine receptor M2-M3 loop. J Biol Chem 280, 35836-35843.

Hidalgo P. and MacKinnon R. (1995) Revealing the architecture of a K+ channel pore through mutant cycles with a peptide inhibitor. Science 268, 307-310.

Huang S. H., Duke R. K., Chebib M., Sasaki K., Wada K. and Johnston G. A. (2003) Bilobalide, a sesquiterpene trilactone from Ginkgo biloba, is an antagonist at recombinant alpha1beta2gamma2L GABA(A) receptors. Eur J Pharmacol 464, 1-8.

Huang S. H., Duke R. K., Chebib M., Sasaki K., Wada K. and Johnston G. A. (2004) Ginkgolides, diterpene trilactones of Ginkgo biloba, as antagonists at recombinant alpha1beta2gamma2L GABAA receptors. Eur J Pharmacol 494, 131-138.

Humphrey W., Dalke A. and Schulten K. (1996) VMD: visual molecular dynamics. J Mol Graph 14, 33-38.

Ivic L., Sands T. T., Fishkin N., Nakanishi K., Kriegstein A. R. and Stromgaard K. (2003) Terpene trilactones from Ginkgo biloba are antagonists of cortical glycine and GABAA receptors. J Biol Chem 278, 49279-49285.

Jaracz S., Nakanishi K., Jensen A. A. and Stromgaard K. (2004) Ginkgolides and glycine receptors: a structure-activity relationship study. Chemistry 10, 1507-1518.

Kneussel M. and Betz H. (2000) Receptors, gephyrin and gephyrin-associated proteins: novel insights into the assembly of inhibitory postsynaptic membrane specializations. J Physiol 525 Pt 1, 1-9.

Kondratskaya E. L., Betz H., Krishtal O. A. and Laube B. (2005) The beta subunit increases the ginkgolide B sensitivity of inhibitory glycine receptors. Neuropharmacology 49, 945-951.

Kondratskaya E. L., Fisyunov A. I., Chatterjee S. S. and Krishtal O. A. (2004) Ginkgolide B preferentially blocks chloride channels formed by heteromeric glycine receptors in hippocampal pyramidal neurons of rat. Brain Res Bull 63, 309-314.

Kondratskaya E. L., Lishko P. V., Chatterjee S. S. and Krishtal O. A. (2002) BN52021, a platelet activating factor antagonist, is a selective blocker of glycine-gated chloride channel. Neurochem Int 40, 647-653.

Le Bars P. L., Katz M. M., Berman N., Itil T. M., Freedman A. M. and Schatzberg A. F. (1997) A placebo-controlled, double-blind, randomized trial of an extract of Ginkgo biloba for dementia. North American EGb Study Group. Jama 278, 1327-1332.

Lynch J. W. (2004) Molecular structure and function of the glycine receptor chloride channel. Physiol Rev 84, 1051-1095.

Lynch J. W., Han N. L., Haddrill J., Pierce K. D. and Schofield P. R. (2001) The surface accessibility of the glycine receptor M2-M3 loop is increased in the channel open state. J Neurosci 21, 2589-2599.

Lynch J. W., Rajendra S., Barry P. H. and Schofield P. R. (1995) Mutations affecting the glycine receptor agonist transduction mechanism convert the competitive antagonist, picrotoxin, into an allosteric potentiator. J Biol Chem 270, 13799-13806.

Maclennan K. M., Darlington C. L. and Smith P. F. (2002) The CNS effects of Ginkgo biloba extracts and ginkgolide B. Prog Neurobiol 67, 235-257.

Miller P. S., Harvey R. J. and Smart T. G. (2004) Differential agonist sensitivity of glycine receptor alpha2 subunit splice variants. Br J Pharmacol 143, 19-26.

Miyazawa A., Fujiyoshi Y. and Unwin N. (2003) Structure and gating mechanism of the acetylcholine receptor pore. Nature 424, 949-955.

Morris G. M., Goodsell, D. S., Halliday, R. S., Huey, R., Hart, W. E., Belew, R. K., and and Olsen A. J. (1998) J. Computational Chemistry 19, 1639-1662.

O'Mara M., Cromer B., Parker M. and Chung S. H. (2005) Homology model of the GABAA receptor examined using Brownian dynamics. Biophys J 88, 3286-3299.

Penzotti J. L., Lipkind G., Fozzard H. A. and Dudley S. C., Jr. (2001) Specific neosaxitoxin interactions with the Na+ channel outer vestibule determined by mutant cycle analysis. Biophys J 80, 698-706.

Pribilla I., Takagi T., Langosch D., Bormann J. and Betz H. (1992) The atypical M2 segment of the beta subunit confers picrotoxinin resistance to inhibitory glycine receptor channels. Embo J 11, 4305-4311.

Sanchez-Crespo M., Fernandez-Gallardo S., Nieto M. L., Baranes J. and Braquet P. (1985) Inhibition of the vascular actions of IgG aggregates by BN 52021, a highly specific antagonist of paf-acether. Immunopharmacology 10, 69-75.

Schreiber G. and Fersht A. R. (1995) Energetics of protein-protein interactions: analysis of the barnase-barstar interface by single mutations and double mutant cycles. J Mol Biol 248, 478-486.

Shan Q., Haddrill J. L. and Lynch J. W. (2001) A single beta subunit M2 domain residue controls the picrotoxin sensitivity of alphabeta heteromeric glycine receptor chloride channels. J Neurochem 76, 1109-1120.

Unwin N. (1995) Acetylcholine receptor channel imaged in the open state. Nature 373, 37-43.

van Beek T. A. (2005) Ginkgolides and bilobalide: their physical, chromatographic and spectroscopic properties. Bioorg Med Chem 13, 5001-5012.

Wang T. L., Hackam A. S., Guggino W. B. and Cutting G. R. (1995) A single amino acid in gamma-aminobutyric acid rho 1 receptors affects competitive and noncompetitive components of picrotoxin inhibition. Proc Natl Acad Sci U S A 92, 11751-11755.

Xu M., Covey D. F. and Akabas M. H. (1995) Interaction of picrotoxin with GABAA receptor channel-lining residues probed in cysteine mutants. Biophys J 69, 1858-1867.

Yan D. and White M. M. (2005) Spatial orientation of the antagonist granisetron in the ligand-binding site of the 5-HT3 receptor. Mol Pharmacol 68, 365-371.

Zhang D., Pan Z. H., Zhang X., Brideau A. D. and Lipton S. A. (1995) Cloning of a gamma-aminobutyric acid type C receptor subunit in rat retina with a methionine residue critical for picrotoxinin channel block. Proc Natl Acad Sci U S A 92, 11756-11760.

Zhao J., Muhammad I., Dunbar D. C., Khan I. A., Fischer N. H. and Fronczek F. R. (2002) Three ginkgolide hydrates from Ginkgo biloba L.: ginkgolide A monohydrate, ginkgolide C sesquihydrate and ginkgolide J dihydrate, all determined at 120 K. Acta Crystallogr C 58, o195-198.

Figure legends

Figure 1. Structures of GA, GB, GC and BB.

Figure 2. Effects of ginkgolides, BB and PTX on α1, α2, α1β and α2β GlyRs. A. Sample currents recorded in response to 10 μM concentrations of the indicated compounds. All traces in each row were recorded from cells expressing the subunits as indicated on the left. Peak current magnitudes in displayed traces ranged from 0.7 - 5 nA. Each current trace is 15 s long. An inward (downward) current was activated by an EC_{50} glycine concentration at around the 2 s mark and this was terminated at 12 s (as indicated by unfilled bar in top left trace), with the test compound being added for a 3-5 s period once the glycine response reached steady-state (filled bar in top left trace). Unless otherwise indicated, all current traces in subsequent figures conform to this protocol. B. Averaged concentration-response curves for GA, GB, GC, BB and PTX. In each of the 5 panels, the α1 GlyR is represented by filled circles, the α2 GlyR by unfilled circles, the α1β GlyR by filled triangles and the α2β GlyR by unfilled triangles. At least 4 full concentration-response relationships were averaged for each compound at each receptor. Averaged IC_{50} and n_H values are summarised in Table 2.

Figure 3. Voltage-dependence of inhibition in the α2 GlyR. A. Sample traces recorded at -40 and +40 mV in the presence of EC_{50} glycine plus either 10 μM GA (left panel) or 10 μM BB (right panel). B. Averaged percentage inhibition induced by each of the indicated compounds at -40 and +40 mV. Each bar represents the average of 3-5 cells.

Figure 4. Glycine concentration-dependence of inhibition in the α2 GlyR. A. Effects of 10 μM GB (left panel) and 10 μM BB (right panel) in the presence of 50 μM (~EC_{50}) glycine and 200 μM (~EC_{100}) glycine. B. Averaged percentage inhibition induced by each of the indicated compounds in the presence of 50 and 200 μM glycine. Each bar represents the average of 3-5 cells.

Figure 5. Use-dependence of inhibition in the α2 GlyR. A. The left panel shows a control where 10 μM GA is applied in the presence of 50 μM glycine. The right panel, from the same cell, shows the effect of a 5 s pre-exposure to 10 μM GA followed immediately by a 50 μM application of glycine. The 'activation' curves, labelled 1, 2 and 3, were fitted with single exponentials. Time constants for curves 2 and 3 were normalised to the curve 1 value. B. Activation time constants for each compound averaged from 4 cells are shown normalised relative to the curve 1 value. All compounds significantly inhibited the glycine activation rate when applied in the open state, but not when applied in the closed state.

Figure 6. GA trap in the $\alpha1^{R271C}$ GlyR. A. All data in A-C were from the same cell. Glycine was applied throughout at 20 mM and GA at 10 μM. Glycine was applied as shown by the unfilled bar, and GA by the filled bar. Note slow recovery from GA inhibition. B. Similar experiment to A except that glycine and GA were simultaneously removed once GA inhibition reached steady-state. Glycine was reapplied 60 s later revealing GA trap. C. GA applied in the closed state does not result in significant trap. D. The mean current amplitude at the 65 s time point is expressed as a percentage of peak control current magnitude for the 3 experimental conditions depicted in panels A-C. The 0 and 65 s time points are shown by the vertical dashed lines. All experiments were averaged from 4 cells, and only experiment B resulted in a significant ($P < 0.05$) current decrease at 65 s.

Figure 7. Modulation of ginkgolide sensitivity by mutations at the 2' and 6' pore-lining positions. A. Sequence alignment of the α1, α2 and β GlyR subunit M2 domains. Residues at the 2' and 6' positions that were mutated in this study are shown in bold. The α1 and α2 subunit sequences differ by a single residue at the 2' position, whereas α and β subunit sequences are poorly conserved. B. Pentameric model of the M2 region of the homomeric α1 GlyR, with the backbone shown as ribbons and the G2' and T6' residues shown as sticks, coloured by atom. The extracellular pore surface is at the top. The best cluster for docking of GA into this structure is shown in gold. C. Sensitivity to all 3 tested ginkgolides was abolished in the homomeric $\alpha1^{T6'F}$ GlyR. All results representative of 4 cells. Ginkgolides were applied at 30 μM and glycine was applied at 50 μM. Note that elimination of

inhibition uncovered a consistent potentiation that may represent a very weak, low efficacy agonist effect at some other site. D. Differential sensitivity of α1β and α2β GlyRs to GA is due to the G2'A substitution. The left panel shows averaged GA dose-response curves in the $\alpha1^{G2'A}$ GlyR, with the corresponding curves for the α1 and α2 GlyRs included as dashed lines for comparison. The right panel shows averaged GA dose-response curves in the $\alpha1^{G2'A}\beta$ GlyR, with the corresponding curves for the α1β and α2β GlyRs included as dashed lines.

Figure 8. Ginkgolide sensitivity changes mediated by the α1 subunit G2'P mutation. Averaged dose-responses of GA, GB, GC and BB in the homomeric $\alpha1^{G2'P}$ GlyR. Corresponding values for the WT α1 GlyR are shown as dashed lines for comparison. Curve parameters of best fit are summarised in Table 2.

Figure 9. Mutant cycle analysis reveals interactions between ginkgolides and the 2' residues of homomeric α1 and heteromeric α1β GlyRs. Mutant cycle analysis of the interaction of GA, GB and GC with: A**.** WT and G2'P mutant homomeric α1 GlyRs and B**.** heteromeric WT α1β and $\alpha1\beta^{P2'G}$ and $\alpha1^{G2'P}\beta^{P2'G}$ heteromeric GlyRs. The Ω values (calculated as in Eq. 1) are shown at the centre of each cycle together with the calculated $\Delta\Delta G_{int}$. Errors in these values were determined by standard propagation of errors using the geometric sum of the relative errors for each IC_{50} value.

Table 1. Functional properties of GlyRs used in this study.

GlyR	I_{max} (nA)	EC_{50} (μM)	n_H	n
α1	4.8 ± 0.8	34.6 ± 1.8	2.0 ± 0.2	9
α2	4.0 ± 1.2	73 ± 6**	1.6 ± 0.2	9
α1β	3.6 ± 0.9	40.3 ± 6.3	1.6 ± 0.2	9
α2β	5.1 ± 1.3	68 ± 4**	2.0 ± 0.2	4
$\alpha1^{T6'F}$ #	0.63 ± 0.05	6.4 ± 1.1*	1.5 ± 0.1	6
$\alpha1^{G2'A}$ #	3.7 ± 0.8	33 ± 1	3.5 ± 0.3	4
$\alpha1^{G2'P}$ #	2.9 ± 0.3	147 ± 27**	2.5 ± 0.3	5
$\alpha1\beta^{P2'G}$ #	4.1 ± 1.2	24 ± 3	2.5 ± 0.2	4
$\alpha1^{R271C}$ @	8.2 ± 2.2	3350 ± 310***	1.8 ± 0.3	12

*** $P < 0.001$ using Student's unpaired t-test.

Results reproduced from Shan *et al.* (2001) and @ Lynch *et al.* (2001).

Table 2. IC_{50} and n_H values for ginkgolides, BB and PTX at WT GlyRs and the homomeric $\alpha^{G2'P}$ GlyR.

compound	α1		α2		α1β		α2β		$\alpha1^{G2'P}$	
	IC_{50} (μM)	n_H	IC_{50} (μM)	n_H	IC_{50} (μM)	n_H	IC_{50} (μM)	n_H	IC_{50} (μM)	n_H
GA	5.9 ± 1.7	-0.87 ± 0.06	11.9 ± 2.9	-0.59 ± 0.07*	9.6 ± 1.4	-0.49 ± 0.07*	1.2 ± 0.4*	-0.93 ± 0.15	183 ± 27**	-0.74 ± 0.04
GB	7.9 ± 1.8	-0.85 ± 0.07	11.4 ± 2.9	-0.61 ± 0.07*	2.5 ± 0.8 $^{*\#\#}$	-0.52 ± 0.05 **	0.8 ± 0.3 ***	-0.79 ± 0.15	49 ± 13$^{*\#}$	-0.50 ± 0.09 $^{*\#}$
GC	10.5 ± 0.8$^{\#}$	-0.97 ± 0.06	10.0 ± 2.2	-1.00 ± 0.27	1.5 ± 0.3$^{***\#\#\#}$	-0.64 ± 0.08 **	0.40 ± 0.09 ***	-0.62 ± 0.05**	4.3 ± 0.6$^{**\#\#}$	-0.59 ± 0.08 *
BB	19.6 ± 1.6$^{\#\#}$	-0.58 ± 0.06$^{\#}$	7.7 ± 2.0**	-0.58 ± 0.08	204 ± 55*	-0.53 ± 0.13	44.9 ± 7.3 $^{*\#\#\#}$	-0.83 ± 0.11	11.9 ± 2.9$^{*\#\#\#}$	-0.85 ± 0.11*
PTX	6.3 ± 0.7	-0.95 ± 0.19	2.3 ± 1.0$^{*\#\#}$	-0.61 ± 0.08	219 ± 28 $^{***\#\#}$	-0.56 ± 0.05	29.7 ± 2.6$^{***\#\#\#}$	-1.31 ± 0.22	2.6 ± 0.6$^{*\#\#\#@}$	-0.90 ± 0.05$^{@}$

$^{*}P < 0.05$, ** $P < 0.01$, *** $P < 0.001$ relative to the corresponding value at the α1 GlyR using Student's unpaired t-test.
$^{\#}P < 0.05$, $^{\#\#}$ $P < 0.01$, $^{\#\#\#}$ $P < 0.001$ relative to the corresponding value for GA at the same GlyR using Student's unpaired t-test.
$^{@}$ Reproduced from Shan *et al*., 2001

Table 3. IC_{50} and n_H values for GA and GB at GlyRs incorporating mutations at the 2' position.

compound	$\alpha1_{G2'P}$		$\alpha1_{G2'P}\beta$		$\alpha1_{G2'P}\beta_{P2'G}$		$\alpha1\beta_{P2'G}$	
	IC_{50} (μM)	n_H	IC_{50} (μM)	n_H	IC_{50} (μM)	n_H	IC_{50} (μM)	n_H
GA	183 ± 27	-0.74 ± 0.04	> 300		> 300		7.1 ± 3.9 ***	-1.00 ± 0.48
GB	49 ± 13	-0.50 ± 0.09	116 ± 23*	-0.81 ± 0.07	162 ± 8***	-0.78 ± 0.05	0.81 ± 0.11*	-0.91 ± 0.14
GC	4.3 ± 0.6	-0.59 ± 0.08	> 300		69 ± 25*	-0.53 ± 0.10	4.3 ± 1.8	-0.56 ± .07

Asterisks represent significance using unpaired Student's t-test relative to the $\alpha1_{G2'P}$ GlyR values. * $P < 0.05$, ** $P < 0.01$, *** $P < 0.001$

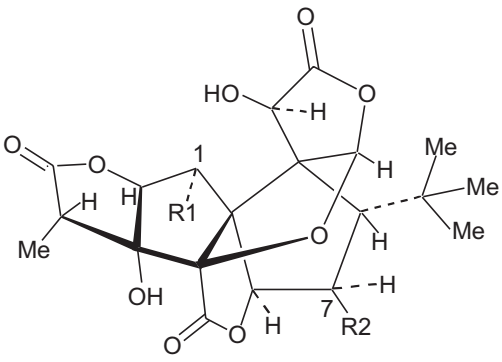

	R1	R2
Ginkgolide A	H	H
Ginkgolide B	OH	H
Ginkgolide C	OH	OH

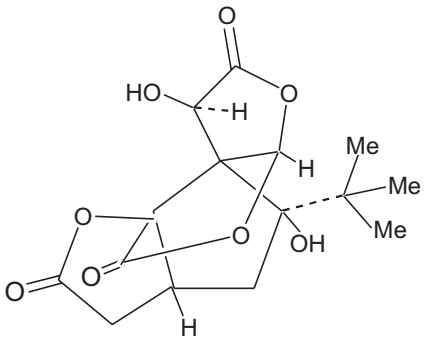

Bilobalide

Figure 1

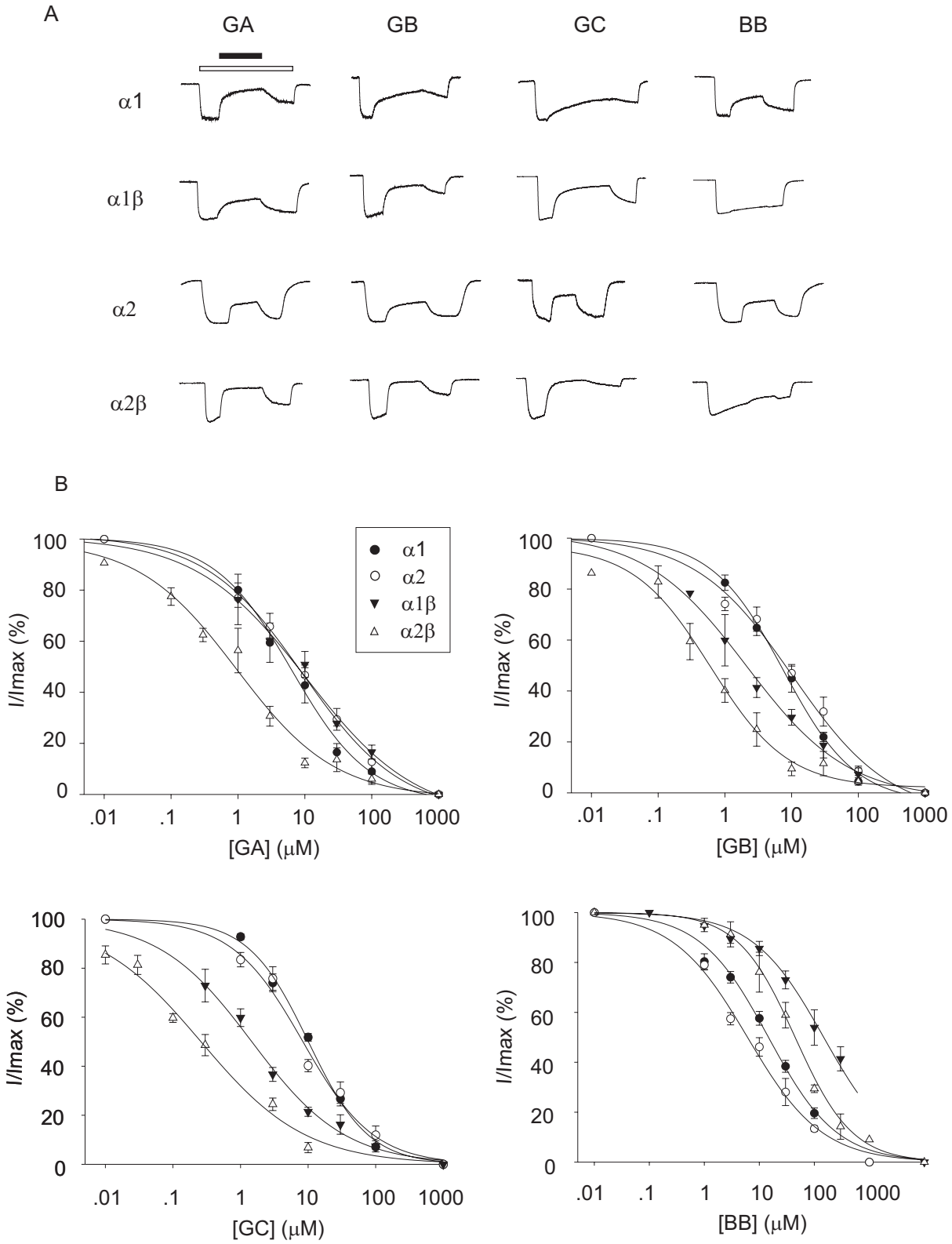
A
GA
GB
GC
BB
α1
α1β
α2
α2β
B
α1
α2
α1β
α2β
I/Imax (%)
[GA] (μM)
[GB] (μM)
[GC] (μM)
[BB] (μM)
0
20
40
60
80
100
.01
.1
1
10
100
1000

Figure 2

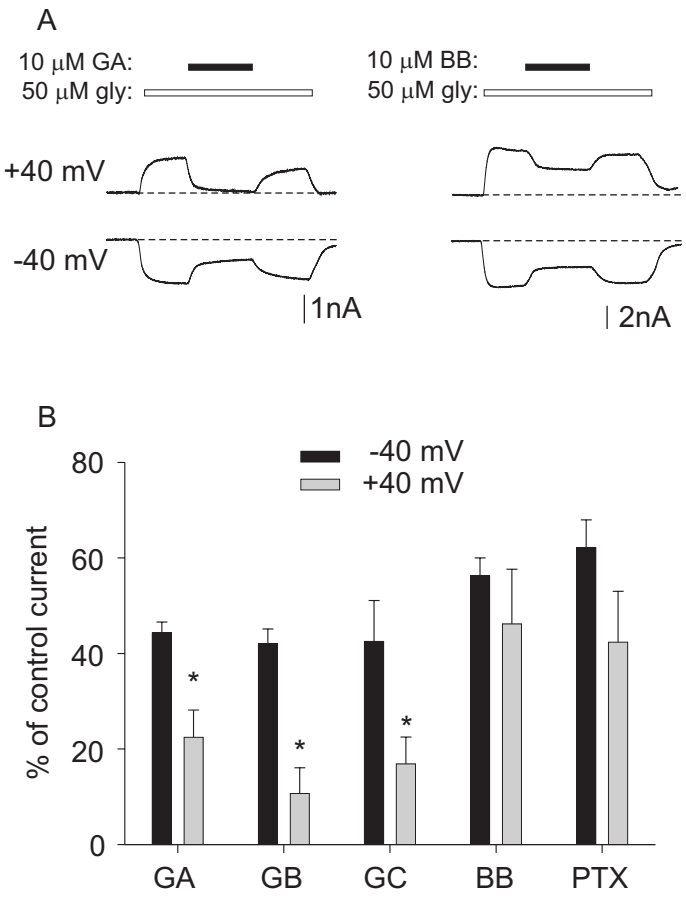
A
10 μM GA:
50 μM gly:
10 μM BB:
50 μM gly:
+40 mV
-40 mV
1nA
2nA
B
-40 mV
+40 mV
% of control current
80
60
40
20
0
*
*
*
GA
GB
GC
BB
PTX

Figure 3

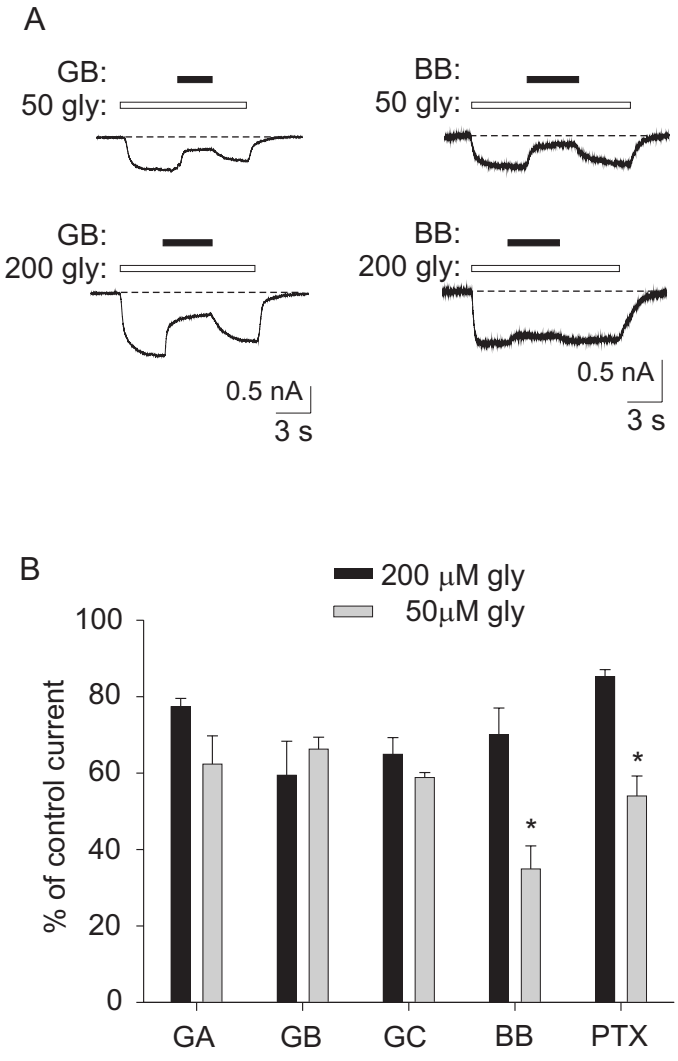
A
GB:
50 gly:
BB:
50 gly:
GB:
200 gly:
BB:
200 gly:
0.5 nA
3 s
0.5 nA
3 s
B
200 μM gly
50μM gly
% of control current
100
80
60
40
20
0
GA
GB
GC
BB
PTX
*
*

Figure 4

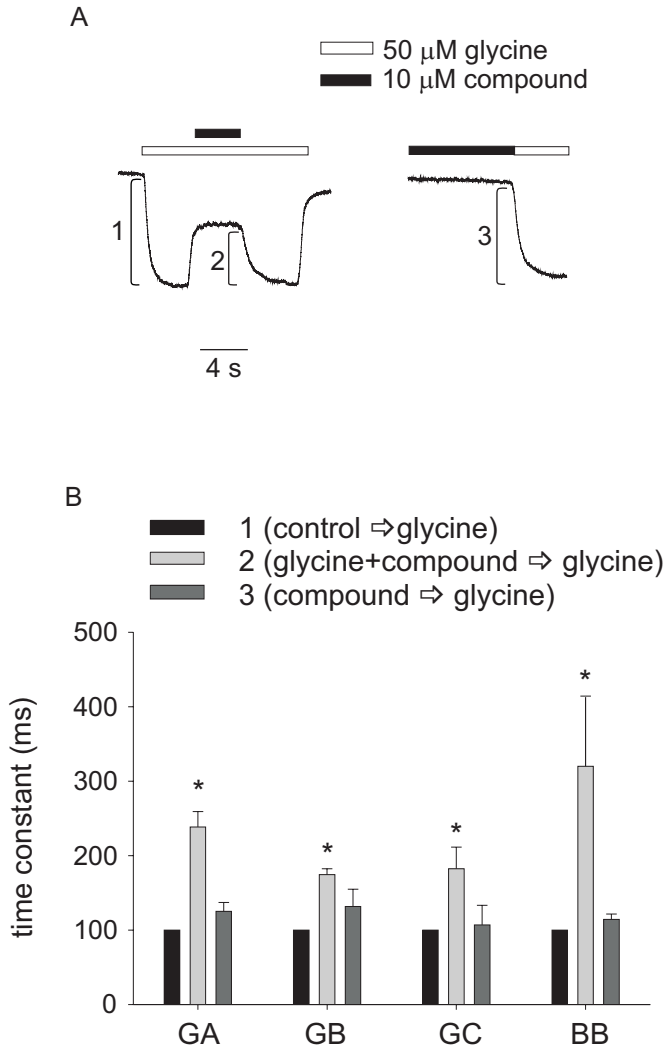
A
50 μM glycine
10 μM compound
1
2
3
4 s
B
1 (control ⇨glycine)
2 (glycine+compound ⇨ glycine)
3 (compound ⇨ glycine)
time constant (ms)
500
400
300
200
100
0
*
*
*
*
GA
GB
GC
BB

Figure 5

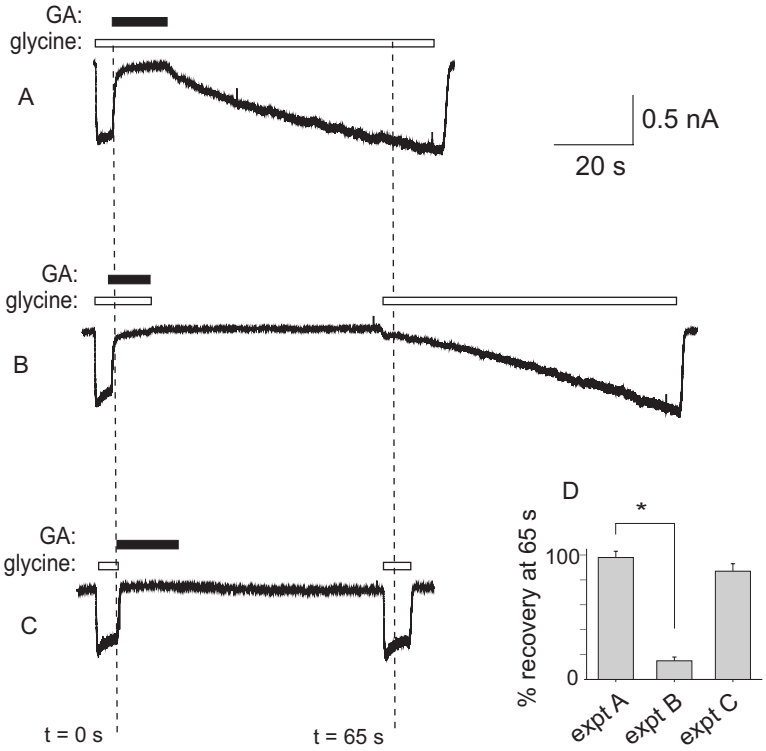
GA:
glycine:
A
0.5 nA
20 s
GA:
glycine:
B
GA:
glycine:
C
t = 0 s
t = 65 s
D
*
% recovery at 65 s
100
0
expt A
expt B
expt C

Figure 6

A

```
                          2′    6′
GlyR α1  250  PARVGLGITTVLTMTTQSSGSR
GlyR α2  257  PARVALGITTVLTMTTQSSGSR
GlyR  β  274  AARVPLGIFSVLSLASECTTLA
```

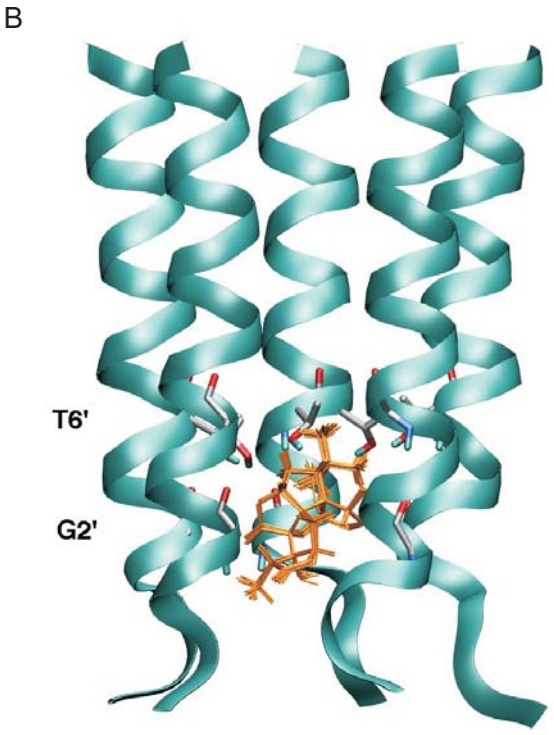

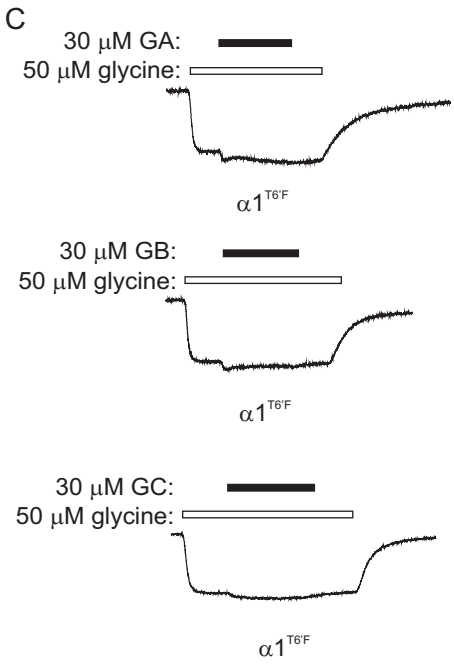

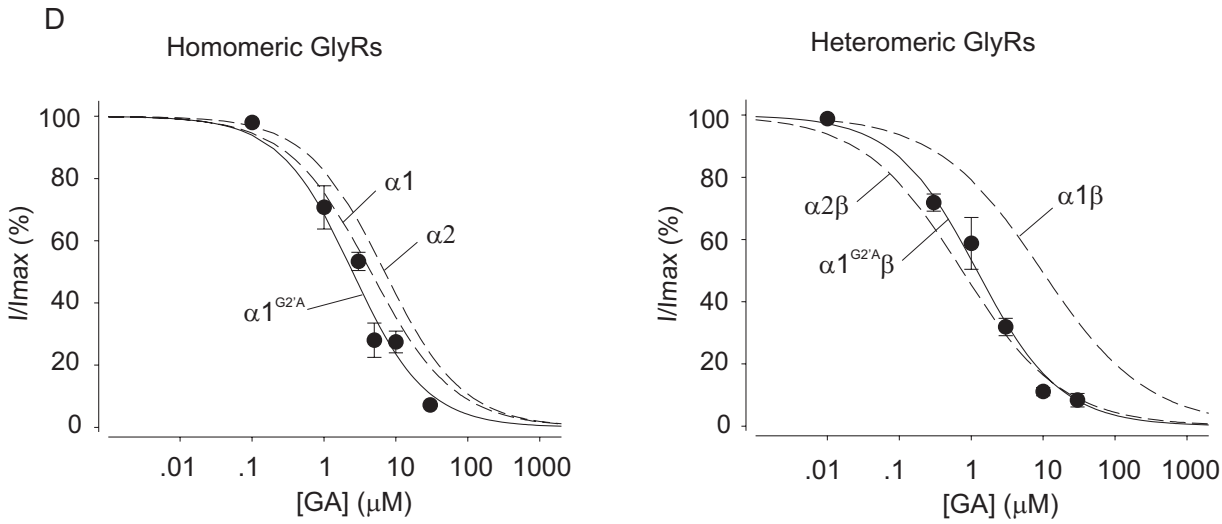

Figure 7

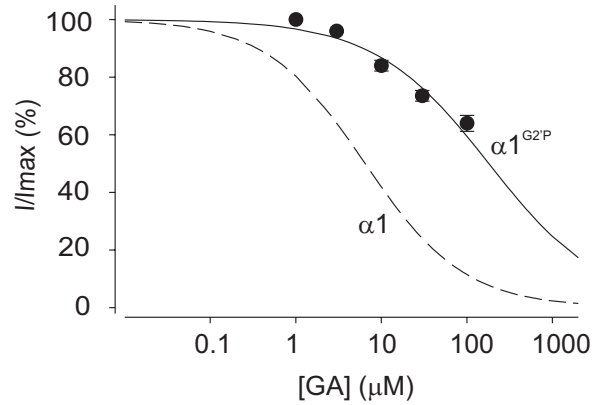
100
80
60
40
20
0
I/Imax (%)
α1G2'P
α1
0.1
1
10
100
1000
[GA] (μM)

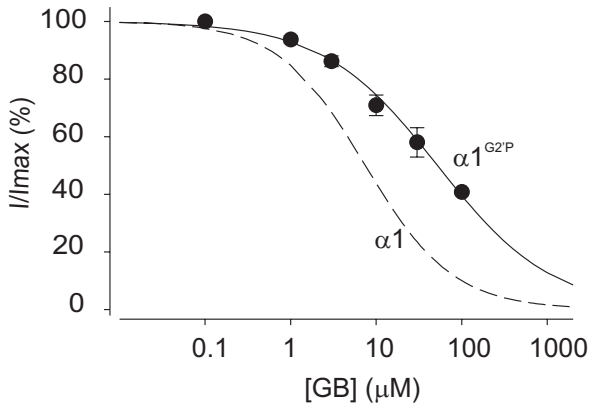
100
80
60
40
20
0
I/Imax (%)
α1G2'P
α1
0.1
1
10
100
1000
[GB] (μM)

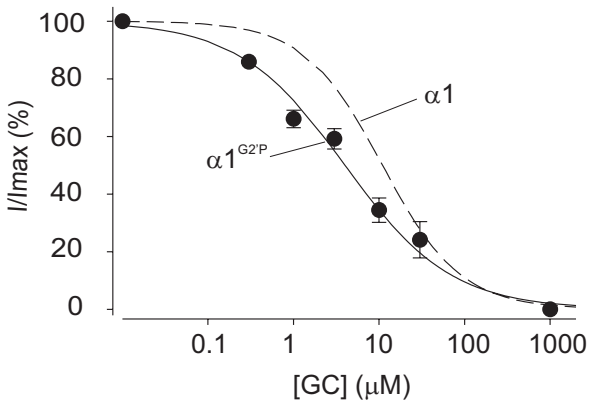
100
80
60
40
20
0
I/Imax (%)
α1
α1G2'P
0.1
1
10
100
1000
[GC] (μM)

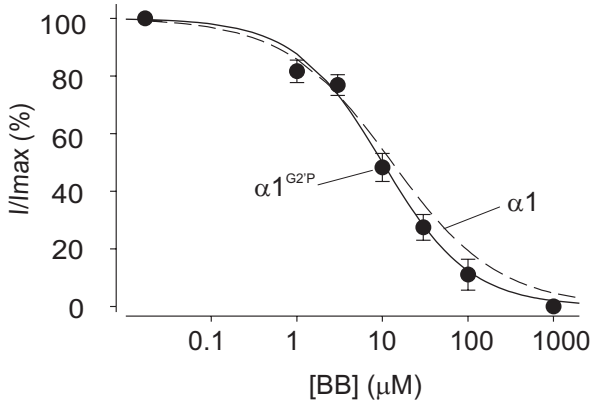
100
80
60
40
20
0
I/Imax (%)
α1G2'P
α1
0.1
1
10
100
1000
[BB] (μM)

Figure 8

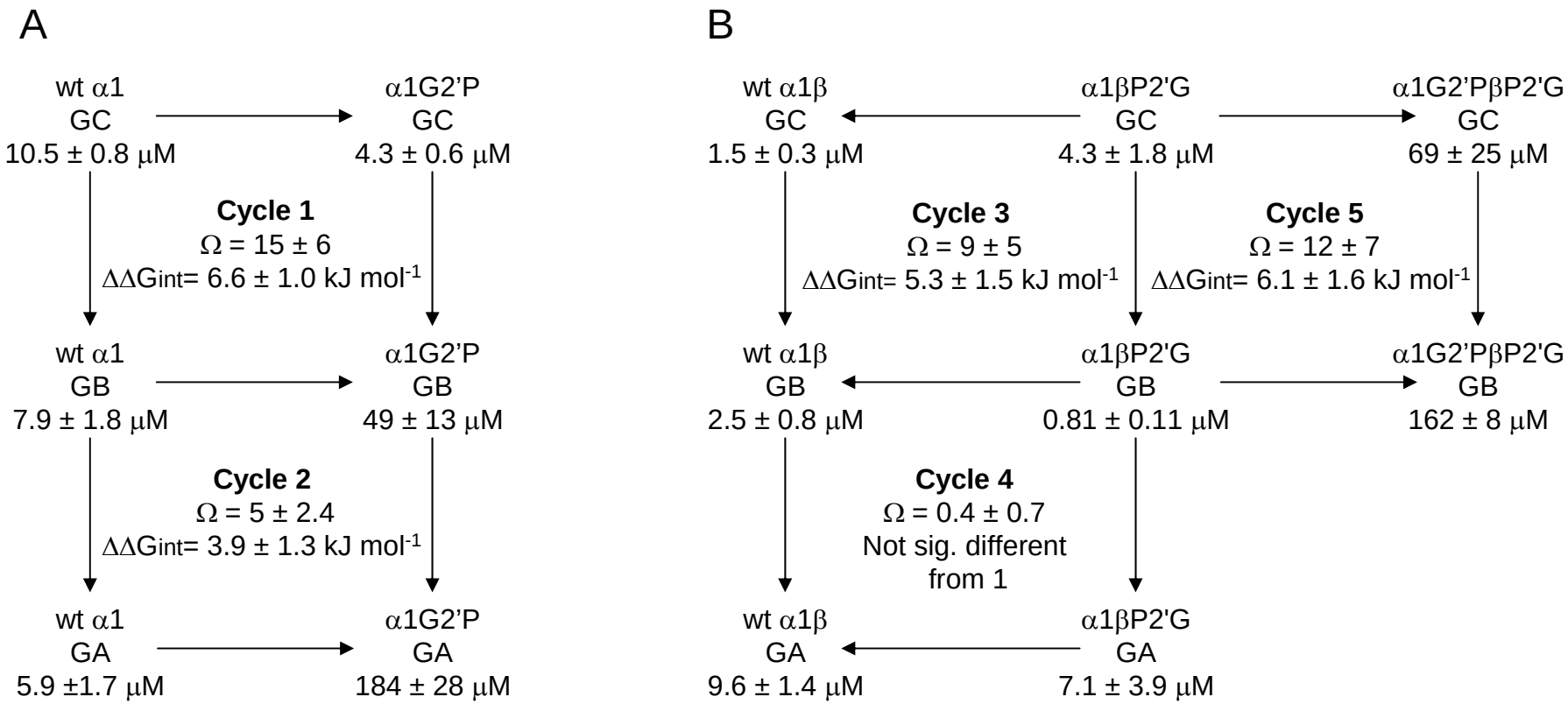
A
wt α1
GC
10.5 ± 0.8 μM
α1G2'P
GC
4.3 ± 0.6 μM
Cycle 1
Ω = 15 ± 6
ΔΔGint= 6.6 ± 1.0 kJ mol-1
wt α1
GB
7.9 ± 1.8 μM
α1G2'P
GB
49 ± 13 μM
Cycle 2
Ω = 5 ± 2.4
ΔΔGint= 3.9 ± 1.3 kJ mol-1
wt α1
GA
5.9 ±1.7 μM
α1G2'P
GA
184 ± 28 μM
B
wt α1β
GC
1.5 ± 0.3 μM
α1βP2'G
GC
4.3 ± 1.8 μM
α1G2'PβP2'G
GC
69 ± 25 μM
Cycle 3
Ω = 9 ± 5
ΔΔGint= 5.3 ± 1.5 kJ mol-1
Cycle 5
Ω = 12 ± 7
ΔΔGint= 6.1 ± 1.6 kJ mol-1
wt α1β
GB
2.5 ± 0.8 μM
α1βP2'G
GB
0.81 ± 0.11 μM
α1G2'PβP2'G
GB
162 ± 8 μM
Cycle 4
Ω = 0.4 ± 0.7
Not sig. different
from 1
wt α1β
GA
9.6 ± 1.4 μM
α1βP2'G
GA
7.1 ± 3.9 μM

Figure 9